

On the properties of HI shells in the Small Magellanic Cloud

D. Hatzidimitriou¹, S. Stanimirovic², F. Maragoudaki³, L. Staveley-Smith⁴,
A. Dapergolas⁵ and E. Bratsolis⁶

¹*Physics Department, University of Crete, P.O. Box 2208, GR 710-03 Heraklion, Crete, Greece*

²*Arecibo Observatory, NAIC/Cornell University, HC 3 Box 53995, Arecibo, Puerto Rico 00612, USA*

³*Section of Astrophysics, Astronomy and Mechanics, Department of Physics, University of Athens, GR-15784 Athens, Greece*

⁴*Australia Telescope National Facility, CSIRO, P.O. Box 76, Epping, NSW 1710, Australia*

⁵*Astronomical Institute, National Observatory of Athens, P.O. Box 20048, GR-11810 Athens, Greece*

⁶*Department Traitement du Signal et des Images, Ecole Nationale Supérieure des Telecommunications, Telecom Paris, 46 rue Barrault, 75634, CEDEX 13, France*

Accepted Received in original form 2003, November 5th

ABSTRACT

There are 509 expanding neutral hydrogen shells catalogued in the Small Magellanic Cloud (SMC), all apparently very young, with dynamical ages of a few Myr. To examine their relationship with young stellar objects we cross-correlated the shell catalogue with various catalogues of OB associations, super giants, Cepheids, WR stars, supernova remnants, and star clusters. The incidence of chance line-ups was estimated via Monte-Carlo simulations, and found to be high. However, it is important that there are 1.5 times more shells that are *not* spatially correlated to an OB association, than shells that are. Moreover, 59 of the 509 shells lie mainly in low stellar density fields and have no young stellar objects associated with them, and therefore no obvious energy source. It is shown that, on the whole, the properties of these “empty” shells are very similar to the properties of the rest of the shells, once selection biases are taken into account. In both cases, the shell radius and expansion velocity distribution functions are consistent with the standard model, according to which shells are created by stellar winds and supernova explosions, as long as all shells were created in a single burst and with a power-law distribution of the input mechanical luminosity. This would indicate a burst of star formation. This interpretation, however, cannot explain why the 59 shells, with no young stellar counterparts, show almost exactly the same behavior as shells with OB associations within their radius. Gamma ray bursts could account for some but certainly not for the majority of the “empty” shells. Many “empty” shells including most of the high luminosity ones, are located in the NW outer regions of the SMC, and may be associated with a chimney-like feature that is known to exist in that area. Finally, it is noted that turbulence is a promising mechanism for the formation of the shell-like structures, but direct comparison with the observations was not possible, at this stage due to lack of detailed models.

Key words:

galaxies: Magellanic Clouds - ISM: bubbles - ISM: kinematics and dynamics

1 INTRODUCTION

High resolution neutral hydrogen (HI) maps of the Small Magellanic Cloud (SMC) (Staveley-Smith et al. 1997, hereafter Paper I) revealed a complex system of more than 500 ‘holes’ surrounded by shells of higher density. Such shells, are common in gas-rich galaxies, and have been catalogued in the Milky Way (e.g. Tenorio-Tagle & Bodenheimer 1988)

as well as in several nearby spirals and irregulars, such as the spirals M31 and M33 (Brinks & Bajaja 1986), the dwarf irregular galaxies IC10 (Shostak & Skillman 1989, Wilcots & Miller 1998), Holmberg II (Puche et al. 1992) and IC2574 (Walter & Brinks 1999) and the Large Magellanic Cloud (LMC) (Kim et al. 1999).

The origin of HI shell-like structures has been the subject of debate for more than two decades, but the issue is

far from settled as yet. Several different mechanisms for HI shell formation have been proposed over the years. They can be classified in the following two main groups.

(i) *Mechanisms that require an energy source central to the shell structure.*

Such mechanisms appear to provide the natural explanation for expanding structures with some spherical symmetry. The assumed energy source could be a single young massive star, or an OB association, or a young star cluster, or some more exotic object such as a gamma-ray burst (GRB).

In the “standard” picture, HI shells result from the combined effect of hot stellar winds from O and B stars and of supernova (SN) shocks (e.g. Weaver et al. 1977; McCray & Kafatos 1987). Already in the 80’s it was recognized (Heiles 1984; Tenorio-Tagle & Bodenheimer 1988) that this explanation could not account for all types of observed structures, especially for rapidly expanding supershells. More recently, high resolution HI velocity maps in Local Group galaxies have greatly revived interest in the subject. For example, in the case of the dwarf irregular galaxy Holmberg II, Rhode et al. (1999) failed to find the remnant stellar populations within the shells that would be consistent with the observed luminosity and age distribution of the shells. Although the energy requirements adopted by these authors may have been significantly overestimated, and hence the limits derived for the necessary remnant populations may be in error (as suggested by Stewart & Walter 2000, and through different reasoning, by Elmegreen & Hunter 2000), there remains the fact that several shells in Holmberg II are actually located in regions of very low optical surface brightness with no indication of recent star formation (see also Bureau & Carignan 2002). As another recent example, we mention the case of the LMC, where no tight correlation was found between HI shells and OB associations (Kim et al. 1999), although many of the shells appeared to be (dynamically) young enough for the presumed OB association to be still recognizable as such. Similarly, a spatially poor correlation between HI shells and OB associations was found recently in the Magellanic Bridge, a tidal bridge of gas between the Magellanic Clouds (Muller et al. 2003). HI shells in the Bridge also appear dynamically much younger than the corresponding OB associations. In the Local Group spirals M31 and M33 again no strong one-to-one correlation has been found between shells and OB-associations, although there are specific examples of HI structures with excellent association with sites of star formation (see review by van der Hulst 1996).

The recent discovery of GRBs led to the realization that such explosive phenomena occurring within a galactic disk would leave rapidly expanding shell-like features in the interstellar medium (ISM), which might account for some of the most luminous shells observed (Loeb & Perna 1998; Efremov et al. 1999; Perna & Raymond 2000). Different authors have proposed different ways of distinguishing shells formed by a GRB or by an OB association (see *Section 4*). Knowledge of the percentage of supershells that are likely to be associated to GRBs, would lead to important constraints on the energetics and rates of GRBs.

(ii) *Mechanisms that do not require a central source.*

One such mechanism involves collisions of high velocity clouds (HVC) with a galactic disk (Tenorio-Tagle 1981;

Tenorio-Tagle et al. 1986), which could reproduce, under specific assumptions, large and energetic features, reminiscent of some of the large HI shell structures in our Galaxy. For example, this mechanism is a possible explanation for the formation of the very luminous “empty” supershell in the Southern Milky Way (McClure-Griffiths et al. 2000).

The non-linear evolution of a self-gravitating disk can also lead to formation of shell-like features, that are not related to a central energy source (Wada & Norman 1999; Wada et al. 2000). Earlier, Elmegreen (1997) also suggested that HI “bubbles” (or shells) could result naturally from the turbulent nature of the interstellar medium, i.e. it is possible that most of the structure of the ISM is the result of natural gaps and holes in the fractal gas distribution caused by turbulence; supernovae, stellar winds, and ionizing radiation partially fill these gaps with hot and warm ionized gas, but they need not structure the ISM much. More recently, Dib & Burkert (2003) used numerical simulations to show that the large-scale turbulence coupled with thermal effects can result in the formation of holes and shell-like features whose sizes are compatible with observations.

Bureau & Carignan (2002) proposed that ram pressure of the intergalactic medium (IGM) must be considered when studying the large and small-scale structure of HI in a low-mass star forming galaxy (in their case, HoII). Ram pressure (of the IGM) can create holes in a dense gaseous disk, as well as enlarge pre-existing holes created by supernova explosions. Unfortunately, no simulations or detailed calculations exist to verify and quantify this process.

Finally, Stewart & Walter (2000) proposed that (pairs of) supershells in spiral (massive) galaxies could result from the localized flaring of a pair of radio lobes formed by jets ejected from the galactic nucleus during an active phase. This mechanism is only mentioned here for completeness, but it obviously does not apply to the SMC case.

All these different processes are not necessarily mutually exclusive and they may well all be taking place, to different degrees of importance. Whichever physical process has resulted into the formation of a certain shell, its subsequent evolution and therefore its observational characteristics (such as its radius, expansion velocity, mass, morphology) get modified by effects that are not related to the origin of the shell. One such effect that has been investigated in detail is radiation pressure from field stars (Elmegreen & Chiang 1982), which can exert an outward force on a large shell of gas and dust in the ISM. This radiative force increases with increasing shell size, so a sufficiently large shell can expand at an ever-increasing speed to a size of 1 kpc or more. This process could obviously attenuate any original differences in the dynamical properties of large, relatively old, shells that actually have different types of origin. Magnetic fields may also alter significantly the shell evolution, but they are not taken into account in current models (e.g. van der Hulst 1996). Metal abundance is also an important constituent of shell evolution, as it affects cooling. Other effects that may modify the evolution of a shell include interactions between neighboring shells, inhomogeneity of the ambient ISM (e.g. McClure-Griffiths et al. 2000), globular cluster passage (Wallin et al. 1996), self-gravity, differential rotation of the galactic disk (e.g. Tenorio-Tagle & Boden-

heimer 1988), as well as ram pressure of the inter-galactic medium, as also noted above.

The rich population of shells in the SMC provides us with an excellent statistical sample with which to re-address some of the basic questions related to the origin and evolution of shells and supershells in gas rich galaxies.

There are over 500 shells and supershells in the SMC (Paper I), five times more than found in the much more massive LMC (Kim et al. 1999). This large number of apparently (dynamically) young shells -apart from being interesting per se, probably pointing towards a recent global burst of star formation in the SMC- provides the ideal data set with which to further investigate the origin of HI shells and supershells, in general. Shell dynamical ages -calculated in the framework of the standard model (see Paper I)- display a very narrow distribution with a mean age of 5.4 ± 0.1 Myr and a standard deviation of 2.8 ± 0.4 Myr. This would imply a highly coherent burst of star formation over the entire main body of the SMC. This high degree of coherence, if real, is not easily explained in the framework of stochastic self-propagating star formation, since the mean shell age is much smaller than the crossing time of a typical shock (see Paper I).

Assuming that the observed HI structures in the SMC are driven by star formation, one would expect to find some correlation between the occurrence and properties of shells and massive star formation activity. The search for such correlations is attempted in Section 2. The statistical significance of these correlations is also examined. In Section 3, we examine the properties of the shells, with the emphasis on the distribution of shells on the expansion velocity - shell radius plane. In Section 4, we discuss the theoretical implications of our results, for the origin and evolution of HI shells. Comparison with different models of shell formation is also attempted. Finally, in the last Section we present our conclusions.

2 ON THE PROJECTED STELLAR CONTENT OF THE HI SHELLS

2.1 The HI shell catalogue

The catalogue of HI shells and super-shells used here is to a large extent identical to the original list published in Paper I, which comprised of 495 giant shells and 6 super-shells. The catalogue included information on the central radial velocity of the shell (V_{hel}), the shell radius (r_s), the shell expansion velocity (v_s), as well as an estimate of the dynamical age (T_s in Myr) of a shell and the wind luminosity required to produce the observed velocity and radius of the shell in the framework of the standard model (see Section 3) for further details). The survey resolution limits were 28 pc for the shell radius, and 1.7 km s^{-1} for expansion velocity.

A re-analysis of the original data, after inclusion of short spacings, led to the discovery of 7 additional shells and three supergiant shells (two of these three supergiant shells were known already but their observational properties have been revised significantly). Properties of the 7 new shells are presented in Table 1, while the properties of the three supergiant shells (one new and two revised) were presented in Stanimirovic et al. (1999). Thus, the total number of HI

shells identified in the SMC has risen to 509. The area covered by the survey was 20 square degrees, and the spatial resolution achieved was 1.6 arcmin (or 28 pc, assuming a distance of 59 kpc).

2.2 Stellar Catalogues

In order to identify possible young stellar counterparts of shells and super-shells, we gathered data on OB associations and star clusters, supergiants, Wolf-Rayet stars, Cepheids and supernova remnants in the SMC.

(i) *OB associations and star clusters*: Bica & Schmitt (1995) carried out a survey of extended objects in the SMC, including OB associations, star clusters, and emission nebulae. Their catalogue contains 1188 objects, of which 554 are classified as star clusters, 343 as associations, and 291 as objects related to emission nebulae.

(ii) *Supergiants and Cepheids*: We compiled a list of 362 young stars (including blue and red supergiants and Cepheid variables) with known positions (precessed to J2000), radial heliocentric velocities and their accuracy and spectral types, based on the catalogues of Maurice *et al.* (1989) and Mathewson *et al.* (1987). Ten of the stars in this list lie beyond the area of the HI observations (with RA greater than $1^{\text{h}}40^{\text{m}}$), and are excluded from further investigation. At the same time, 171 out of the 509 shells lie beyond the area covered by the stellar list we have compiled. This list was treated differently from the other catalogues described in this Section, because it includes information on the radial velocity of the stars. As will be shown later, radial velocity can be used as a discriminator against chance line-ups.

(iii) *Wolf-Rayet stars*: Wolf-Rayet (WR) stars generally have winds significantly stronger than those of their OB stellar progenitors. Only 9 WR stars have been identified in the SMC, and the coordinates were taken from the corresponding discovery papers (Azzopardi & Breysacher 1979; Morgan et al. 1991).

(iv) *Supernova remnants*: We used the catalogue of 25 known and candidate supernova remnants given by Filipovic et al. (1998). For 12 of these supernova remnants, we used the more accurate coordinates provided in Wang & Wu (1992).

Supplementary information on the spatial distribution of young stellar populations in the SMC was derived from the analysis of stellar populations in the SMC by Gardiner & Hatzidimitriou (1992), by Maragoudaki et al. (2001) and by Harris & Zaritsky (2004). Finally, because the completeness of the various catalogues used was probably not uniform, and difficult to assess, we also conducted an independent survey for OBA spectral types based on UK Schmidt Telescope Objective Prism plates (see following paragraph).

2.3 Correlation Results

The catalogue of the 509 shells and super-shells (Section 2.1) was correlated with the catalogues described in Section 2.2 in order to identify objects that are spatially associated with the shells, and therefore likely to be related to their formation. Any object with coordinates lying within the radius of a particular shell was regarded as a possible related source.

Table 1. List of positions, radii, heliocentric velocities, expansion velocities, ages and required wind luminosities for seven new giant and supergiant shells (Stanimirovic S., PhD Thesis, 1999). These add to the 501 shells in Staveley-Smith et al. (1997) (two of which have properties modified by Stanimirovic et al. (1999)) and one new shell listed in Stanimirovic et al. (1999), giving 509 shells altogether.

Supergiant Shell	RA (J2000)	DEC (J2000)	Shell Radius r ($'$) (pc)	Heliocentric Velocity V_{hel} km s^{-1}	Expansion Velocity v_s km s^{-1}	Age T_s (10^6 yr)	Wind Luminosity $\log(L_s/n_0)$ ($L_\odot \text{ cm}^3$)
34A	00:40:06	-71:28:16	20	342	141	21	4.9
84A	00:44:23	-72:26:18	18	313	148	20	4.8
182A	00:52:34	-72:26:55	19	337	151	18	4.7
198A	00:53:58	-73:00:59	12	205	150	34	5.1
389A	01:10:50	-73:35:30	18	315	186	24	5.0
394A	01:11:59	-72:22:28	18	321	191	16	4.5
411A	01:14:32	-72:54:40	16	281	163	24	4.9

* The great majority of the shells were found to have at least one such correlation. There are 200 shells that appear to be spatially associated with at least one OB association, 241 shells with at least one star cluster, 71 with at least one star from the young star catalogue, 18 with at least one WR star and 41 with at least one SNR. However, because of the large stellar density, it is more than likely that a significant percentage of these correlations is only due to chance line-ups. Indeed, Monte-Carlo simulations showed that $\simeq 85\%$ of spatial correlations found in this way fall into this category. This result suggests that it is difficult to derive meaningful conclusions about the origin of shells from spatial-only correlations. In order to reduce the incidence of false correlations, one can impose a radial velocity constraint as well, retaining only correlations for which the radial velocities of shell and object agree, for example, to within one-sigma of the combined velocity error. Such a procedure was only possible for the second catalogue of Section 2.2, which includes radial velocity information. It was found that only 21% of the spatial correlations found between shells and catalogue objects also satisfied the radial velocity criterion. This low percentage emphasizes the high incidence of chance line-ups, also suggested by the Monte-Carlo simulations. It becomes obvious that the high stellar density precludes the identification of objects that could be -with some certainty- considered to be linked with the power source of a particular shell. The variable size of the shells further complicates the issue, introducing additional selection biases. Radial velocity information would provide a useful tool, but unfortunately, the catalogue of young objects with radial velocity values is far too incomplete. What is remarkable, however, is that 80 shells, i.e. 16% of the total population, have no young objects, from any of the catalogues of Section 2.2, lying within their radius. The case of OB associations is of particular interest as they are often thought to be the power source of HI shells: *there are 1.5 times more shells that are not spatially correlated to an OB association than shells that are.*

This is the first indication that some of the shells may

* The use of the radius to define the spatial limit of a shell, implicitly assumes that the shells are spherical. This assumption could only critically affect the resulting associations for small shells. However, small shells, particularly of Group II (see below), are nearly circular in appearance. Therefore, our assumption is not expected to affect significantly our results, regarding the nature of "empty" and "non-empty" shells.

not be directly related to young stellar objects, although -as it will be seen in Section 3- they appear to be dynamically as young as the rest of the shells. However, it can be argued that there may be isolated young stars (of OB and A spectral types) within these apparently "empty" shells, as the catalogues used are not necessarily complete. In order to isolate the shells that are indeed empty of young stars, we searched within these 80 shells for OB and A spectral-type stars. The spectral classification was performed by visual inspection (through a microscope) of low and medium dispersion objective prism plates, taken with the UK 1.2m Schmidt Telescope. OB and A spectral types are very easy to identify on these plates (Savage et al. 1985a; Savage et al. 1985b; Kontizas et al. 1988). There are two advantages in performing this classification: (i) the observational material, and the identification method are uniform for all shells; (ii) we cover the outer regions of the SMC, which were unevenly covered by the catalogues of Section 2.2. Actually, exactly because of the low stellar density in these areas, spectral classification is expected to give quite accurate results (for bright stars). The conclusion of this exercise is that 59 of the 80 previously identified shells, are indeed empty of young stellar counterparts. In Table 2 we provide the list of these 59 shells -along with their properties (columns as in Table 1).

3 SHELL PROPERTIES

Following the results of the previous Section, the HI shells are classified into two groups: Group I, which contains the 450 shells with some young stellar counterpart; Group II, which contains the 59 "empty" shells of Table 2. The shell properties are examined separately for Group I and Group II members.

The basic observational properties of the shells, that will be explored, also in relation to their stellar content, include the shell radius (r_s), and expansion velocity (v_s) as described in Section 2.1, as well as morphological characteristics of shells of particular interest (see below). Apart from these properties, which come directly from the data cubes without any assumptions, we also refer to two derived quantities, namely, the dynamical age ($T_s = \frac{3}{5}r_s/v_s$ in Myr) of a shell and the (logarithm of the) wind luminosity required to produce the observed radius and expansion velocity ($\log L_s/n_o$), where n_o is the ambient ISM density

Table 2. List of positions, radii, heliocentric and expansion velocities, dynamical ages and required wind luminosities for Group II (empty) shells

Shell	RA J	DEC 2000	Shell Radius r_s pc	Heliocentric Velocity V_{hel} $km\ s^{-1}$	Expansion Velocity v_s $km\ s^{-1}$	Dynamical Age T_s $10^6\ yr$	Wind Luminosity $\log(L_s/n_0)$ $L_\odot\ cm^3$
11	00:34:52	-72:31:19	104.6	138.9	14.4	4.3	3.4
14	00:35:14	-73:06:06	32.6	119.5	10.2	1.9	1.95
17	00:35:40	-71:23:34	116.6	155.9	16.1	4.3	3.64
18	00:36:19	-71:19:17	53.2	144.1	6.2	5.2	1.74
21	00:37:13	-70:59:55	199.0	137.3	26	4.6	4.73
25	00:38:30	-71:41:21	116.6	136.5	14.4	4.8	3.49
29	00:39:12	-71:24:56	209.3	144.1	33.5	3.7	5.11
34	00:40:02	-74:59:47	48.0	135.0	2.9	9.8	0.65
36	00:40:26	-71:13:13	99.5	139.7	17.6	3.4	3.62
37	00:40:26	-72:58:52	18.9	112.8	2.9	3.9	-0.15
40	00:40:40	-70:45:58	99.5	139.2	14.7	4	3.38
44	00:41:20	-74:19:55	89.2	163.3	3.8	14.1	1.52
50	00:41:40	-70:50:50	53.2	124.6	5.0	6.3	1.45
51	00:41:40	-71:07:32	22.3	115.8	1.7	8.1	-0.71
54	00:41:57	-73:06:48	29.2	169.1	2.5	6.6	0.01
56	00:42:07	-73:00:50	18.9	114.0	6.7	1.7	0.93
58	00:42:22	-71:42:35	147.5	141.8	20.8	4.2	4.18
59	00:42:25	-75:15:13	221.3	152.4	10	13.2	3.57
60	00:42:33	-74:03:48	34.3	113.2	5.9	3.5	1.27
69	00:43:14	-71:26:10	58.3	158.1	8.1	4.3	2.14
71	00:43:34	-72:41:40	17.2	150.1	1.8	5.4	-0.87
75	00:43:40	-71:33:50	29.2	168.2	3.0	5.8	0.23
76	00:43:46	-72:32:41	27.4	160.6	2.9	5.4	0.15
78	00:44:00	-72:28:14	60.0	143.3	18.1	2.0	3.21
84	00:44:23	-71:29:29	33.0	131.9	4.8	4.2	0.96
85	00:44:27	-71:40:5	30.9	129.1	2.9	6.2	0.25
89	00:44:46	-74:17:42	66.9	132.6	4.5	8.8	1.51
94	00:44:58	-74:25:11	37.7	134.3	2.1	10.9	0.01
105	00:45:58	-72:39:09	34.3	125.2	8.8	2.3	1.79
112	00:46:36	-74:43:18	77.2	135.9	7.6	6.0	2.3
119	00:47:01	-74:34:27	96.1	96.6	11.2	5.1	3.0
140	00:49:05	-71:30:20	20.7	153.6	2.2	5.6	-0.45
146	00:49:21	-71:40:56	56.6	154.8	8.4	4.0	2.16
155	00:50:15	-71:19:53	34.3	161.6	4.6	4.4	0.95
166	00:51:15	-71:23:00	49.7	160.0	6.2	4.8	1.67
175	00:51:34	-71:15:27	53.2	157.0	5.9	5.5	1.66
182	00:52:26	-71:10:58	41.2	151.0	2.9	8.4	0.53
211	00:54:48	-71:12:33	108.1	151.9	8.8	7.3	2.79
214	00:55:03	-71:06:30	32.6	159.0	2.9	6.7	0.33
221	00:56:01	-72:11:25	20.6	160.4	2.2	5.6	-0.47
225	00:56:24	-70:48:17	12.0	117.7	1.5	5.1	-1.42
229	00:56:47	-71:39:44	17.1	156.8	1.5	7.1	-1.14
234	00:57:04	-71:35:12	46.3	156.1	3.7	7.3	0.91
277	01:00:26	-71:06:10	24.0	162.6	4.0	3.7	0.50
286	01:00:49	-71:13:42	32.6	156.4	4.0	4.9	0.75
289	01:01:12	-71:10:37	75.5	173.4	11.4	3.9	2.80
302	01:02:11	-71:07:26	53.2	165.1	5.5	5.8	1.57
314	01:03:50	-74:41:45	22.3	152.9	2.3	5.9	-0.35
369	01:08:53	-71:24:03	37.7	117.7	2.6	8.7	0.26
385	01:10:26	-71:12:56	22.3	145.2	4.2	3.3	0.48
422	01:15:11	-71:06:29	15.4	175.5	1.7	5.5	-1.07
441	01:17:32	-71:08:24	116.6	191.2	13.6	5.1	3.42
452	01:19:04	-72:05:19	46.3	186.0	10.9	2.5	2.32
459	01:20:05	-74:35:18	42.9	185.3	5.4	4.6	1.34
466	01:20:48	-74:40:57	90.9	183.9	4.6	11.9	1.80
473	01:21:45	-71:21:19	25.7	206.6	2.9	5.1	0.08
476	01:22:46	-71:54:10	70.3	189.3	12.0	3.5	2.81
486	01:24:32	-74:39:05	56.6	188.3	7.1	4.8	1.96
493	01:26:32	-71:53:17	248.7	205.2	9.6	15.4	3.63

(in cm^{-3}). The wind luminosity, $\log L_s$, is only meaningful in the framework of the "standard" model. The formulae used for the derivation of these quantities and the inherent assumptions are described in Paper I.

Morphologically, both groups of shells show similar general properties: larger shells are usually not well defined and have only partially visible rims, while smaller shells are better defined and often show up as small donuts in a few consecutive channels and then quickly disappear.

3.1 Spatial distribution of Group I and Group II shells

Figure 1 shows the spatial distribution of all 509 shells. Filled circles mark the positions of Group I shells, Group II shells are denoted by crosses, while the 7 most luminous Group II shells are indicated by open squares (see Section 3.4).

The spatial distribution of Group I shells follows the HI distribution (indicated with contours in Figure 1), which

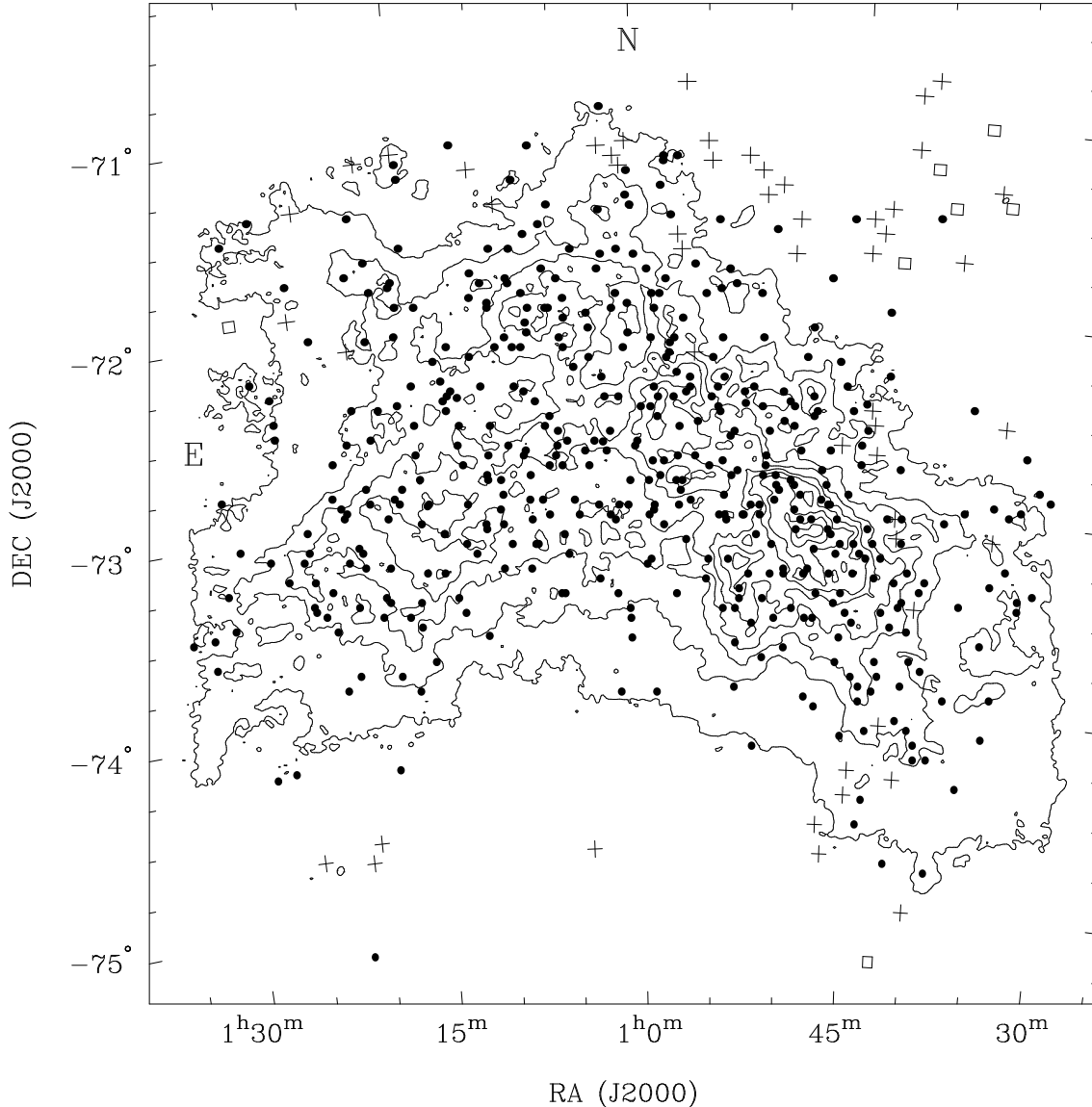


Figure 1. Spatial distribution of the centers of HI shells in the SMC superimposed on contours of the HI integrated column density. The contour interval is 1.4×10^{21} atoms cm^{-2} and contours at $1\text{--}10 \times$ contour interval are shown. Filled circles represent Group I shells while crosses represent Group II shells. Open squares show the Group II with high luminosity, which are discussed in Section 3.4.

expectedly coincides with the distribution of young populations in the SMC (Maragoudaki et al. 2001, Harris & Zaritsky 2004). The highest concentration of Group I objects is thus found along the Bar and the Wing, with the density of objects falling progressively in the outer regions. On the other hand, Group II shells are mostly outliers, located beyond the second to last contour of Figure 1. Indeed for these shells we would not expect to find young stellar counterparts, as they are located in regions that are known to host only intermediate and old populations (see e.g. Gardiner & Hatzidimitriou, 1992 and Harris & Zaritsky, 2004).

The histograms of Figure 2 show clearly that indeed there is a lack of Group II shells in the inner regions. This can be at least partly explained by the fact that high stellar density would prohibit discovery of “empty” shells in the inner, crowded regions. On the other hand, one might inter-

pret this difference as indicating that the empty shells are mainly older. However, as we shall see in paragraphs 3.1 and 3.2, there is no difference in the dynamical ages of the two groups of shells.

It is also noteworthy that there is a significant population of Group II shells lying in the Northwestern outer regions of the SMC. Actually, about half the Group II shells (29) are located within a limited area with $0.59 < RA < 1.04$ and $-71.7 < Dec < -70.8$, in the NW. These NW Group II shells will be further discussed in the following paragraphs.

3.2 Differential shell radius and expansion velocity distribution functions

The shell radii, r_s , range from close to the resolution limit of the survey to 473 pc, with a mean value of 93pc. The

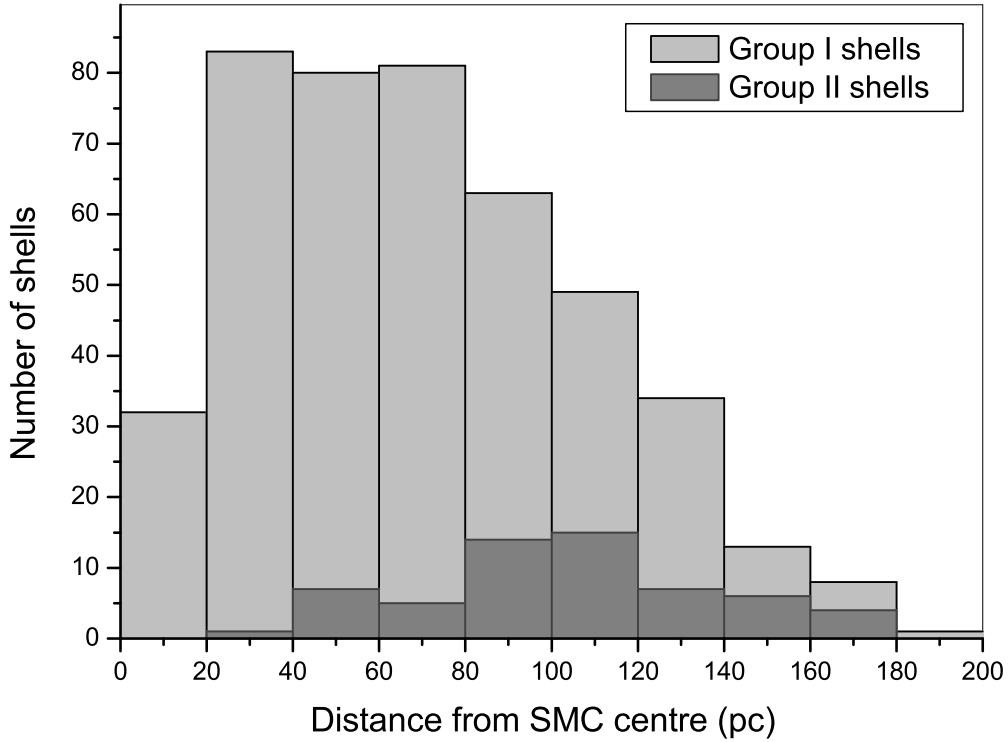


Figure 2. Histograms of the distances from the SMC centre for Group I (light grey) and Group II (dark grey) shells

expansion velocities, v_s , range from close to the resolution limit to $\simeq 33.5 \text{ km s}^{-1}$, with a mean value of 10.3 km s^{-1} . Thus, in many cases v_s is a significant fraction of the SMC escape velocity of $\simeq 50 \text{ km s}^{-1}$. This suggests that the ISM of the SMC is suffering from severe disruption, a result that is also indicated by the fact that the total wind energy of the catalogued shells deposited in the ISM is a significant fraction ($\simeq 5\%$) of the total HI+He binding energy in the SMC (Paper I).

Figure 3 shows the differential distribution functions of the shell radii, $N(r_s)$, and expansion velocity, $N(v_s)$, for Group I and empty Group II shells[†]. The shell radius and expansion velocity distributions peaks are given in Table 3. Group I and Group II distributions peak at significantly different values, with Group II shells appearing in general smaller and with lower expansion velocities than Group I shells. More than two thirds of empty shells have $r_s < 100 \text{ pc}$ and $v_s < 10 \text{ km s}^{-1}$. It must be emphasized however, that chance line-ups increase with increasing shell size. Therefore, the lack of larger, faster expanding shells of Group II can be at least partly attributed to selection biases. On the

other hand the relative paucity of small non-empty (Group I) shells appears to be real.

Over much of the range, $N(r_s)$ and $N(v_s)$ can be fitted by a power-law, $N(r_s) \propto r_s^{\alpha_{rs}}$ and $N(v_s) \propto v_s^{\alpha_{vs}}$. The fit in each case has been statistically weighed (by the inverse of the root-N errors shown on Figure 3). The derived exponents and the corresponding error bars are presented in Table 3. The values of α_{rs} depend on the bin size used to derive the distribution functions of Fig.3. Expectedly, varying the bin size leads to different exponents, which, however, are in agreement with each other within the quoted errors. On the other hand, the derived exponents also depend quite sensitively on the choice of the minimum shell radius and expansion velocity ($r_{s,\min}$ and $v_{s,\min}$) for the data used for fitting. This difference is at least partly due to the different level of completeness of the bins for small shells, but it could also be caused by deviations from the derived single exponent law, for smaller shells. The resolution limit of the survey is 28pc. Considering shells larger than twice this limit (i.e. larger than 60pc), we obtain an exponent of $\alpha_{rs} = -2.46 \pm 0.13$ (for Group I shells), while, considering shells larger than 100pc (as done by OC97), which is more than three times the resolution limit, we get $\alpha_{rs} = -2.7 \pm 0.2$ (for Group I shells), in agreement with the result of OC97.

[†] For the expansion velocity distribution functions, we use

[‡] This result, is identical to the result of OC97, as would be

[†] Although we do not show here the differential distribution functions for all shells (Group I and Group II together), these are almost identical to the Group I plots and very similar to those published by Oey and Clarke (1997), as would be expected since the samples are almost identical.

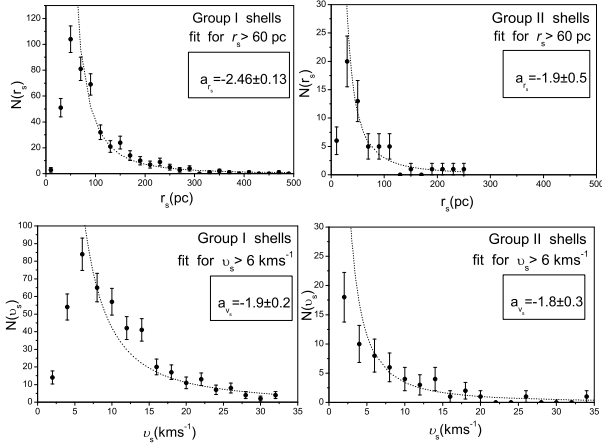


Figure 3. The differential distribution functions of shell radius and expansion velocity for the Group I (left panels) and for Group II shells (right panels). Statistical errors, $N^{1/2}$ are shown. The weighted power-law fits, $N(r_s) \propto r_s^{\alpha_{rs}}$ and $N(v_s) \propto v_s^{\alpha_{vs}}$ are overlaid. All slopes are listed in Table 3.

two different values of $v_{s,\min}$, at 6 and 8 km s^{-1} , in accordance with the limits in shell radius r_s . For $v_{s,\min} = 6 \text{ km s}^{-1}$, the exponent of the power-law is $\alpha_{vs} = -1.8 \pm 0.2$, while it becomes -2.1 ± 0.2 for $v_{s,\min} = 8 \text{ km s}^{-1}$. All these values refer to Group I shells.

The same procedure is followed for Group II shells (Table 3).

The least-squares power-law fits that are shown in Figure 3, are those derived with $r_{s,\min} = 60 \text{ pc}$ and $v_{s,\min} = 6 \text{ km s}^{-1}$.

As it can be seen in Table 3, all slopes are between -1.8 and -2.9. Slopes derived using different lower limits are in all cases in good agreement with each other, within the combined errors. Also, $\alpha_{rs} \simeq \alpha_{vs}$ (within the combined errors) for all cases. Group I and Group II shell distributions can be described by very similar power law fits (for the adopted limiting radii and expansion velocities).

3.3 Distribution on the $\log v_s - \log r_s$ plane

Figure 4 shows the locus of Group I and Group II shells on the $\log v_s$ vs $\log r_s$ plane. Both groups of shells occupy a similar area on the $\log v_s$ vs $\log r_s$ plane, although most small shells belong to Group II, as noted earlier. The solid line is the least absolute deviation fit to all Group I shells, having a slope of 0.68 ± 0.03 . The dashed line is the corresponding

expected, however the quoted error is significantly smaller in our case. This is due to the fact that we quote standard errors, while OC97 quoted rms values).

§ The expansion velocity limits have been chosen so that the point $[r_{s,\min}, v_{s,\min}]$ lies close to the mean line defined by the data points on the r - v plane. This was considered to be necessary, since the resulting exponents for the radius and velocity distributions are subsequently inter-compared

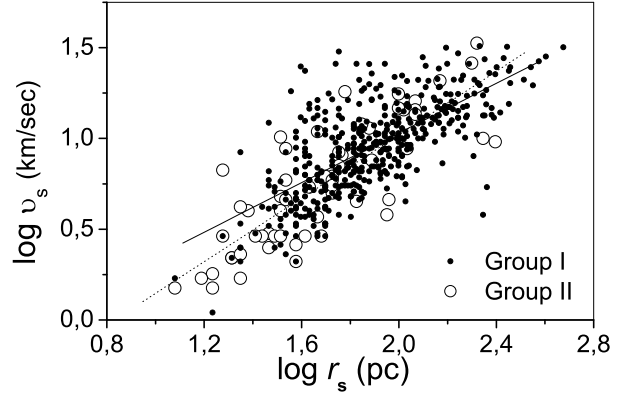


Figure 4. The logarithm of expansion velocity (in km s^{-1}) versus the logarithm of shell radius (in pc) for the entire sample of HI shells. Filled circles mark Group I ("non-empty") shells, and open circles mark Group II ("empty") shells. The solid line is the least absolute deviation fit to Group I shells, while the dashed line to Group II shells.

line for the Group II shells, and has a slope of 0.87 ± 0.08 . The slopes derived for the two Groups of shells differ by about twice the combined errors. For all 509 shells, the corresponding slope is equal to 0.71 ± 0.03 , i.e. very similar to the Group I slope.

The scatter around the regression lines shown in Fig.4 is quite large especially for Group I shells, at intermediate radii. It would appear that most small shells lie below the regression lines (regardless of group), pointing towards a different slope for the smaller shells. Indeed, if we consider only shells with $\log r_s < 1.6$ (of both groups), the slope of the corresponding regression line approaches unity (0.95 ± 0.09), indicating a linear relationship between v_s and r_s . For larger shells ($\log r_s \geq 1.6$), on the other hand, the slope appears to be lower at (0.58 ± 0.05). This difference is statistically significant at the 3-sigma level and it may account at least partly for the difference between the slopes for Group I and Group II, since the proportion of small shells is larger within the Group II objects. Indeed, if we only take into account shells with $\log r_s > 1.6$, the slopes of the two groups agree within one-sigma.

The implications of these results will be further discussed in the following sections.

3.3.1 Effect of distance from the SMC center

We now examine whether the distribution of Group I and Group II shells on the $\log v_s$ vs $\log r_s$ plane depends on the projected distance of a shell from the kinematic center of the SMC (at RA $00^{\text{h}} 51^{\text{m}}$, Dec -73° , 1950). We divided each group into two subgroups, the "inner" and "outer". The former includes shells at (projected) distances smaller than 50 arcmin (i.e. $\simeq 0.85 \text{ kpc}$) from the SMC center and the latter at distances larger than 1.5 degrees (i.e. $\simeq 1.55 \text{ kpc}$). Figure 5 shows the differences in the distribution of the two subgroups on the $\log v_s$ vs $\log r_s$ plane, for Group I and Group II shells (top and bottom panel respectively).

Table 3. The number of shells, the peak of the shell radii distribution (for the entire sample of the particular shell type), the lower limit adopted for the power-law fit, and the resulting exponent of the power law (followed by the standard error), followed by the same parameters for the shell expansion velocity distribution.

Shell Type	N_{shells}	Radius			Expansion velocity		
		Peak (pc)	Lower Limit $r_{s,\text{min}}$ (pc)	Slope α_{r_s}	Peak (km s ⁻¹)	Lower Limit $v_{s,\text{min}}$ (km s ⁻¹)	Slope α_{v_s}
All shells	509	$\simeq 60$	60	-2.39 ± 0.12	$\simeq 8$	6	-2.0 ± 0.2
All shells			100	-2.7 ± 0.2		8	-2.4 ± 0.2
Group I	450	$\simeq 60$	60	-2.46 ± 0.13	$\simeq 8$	6	-1.9 ± 0.2
Group I			100	-2.8 ± 0.2		8	-2.4 ± 0.2
Group II	59	$\simeq 30$	60	-1.89 ± 0.45	$\simeq 3$	6	-1.8 ± 0.3
Group II			100	-2.9 ± 1.4		8	-2.3 ± 0.3

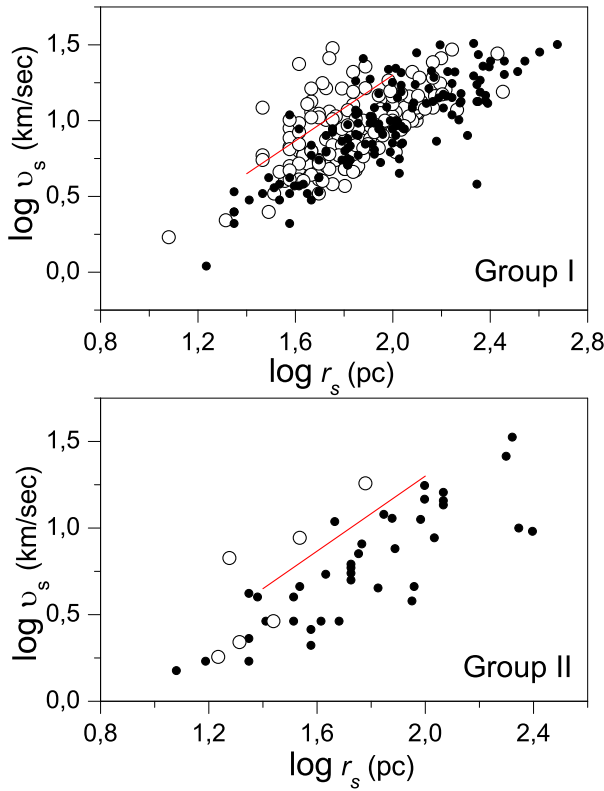


Figure 5. The logarithm of expansion velocity (in km s⁻¹) versus the logarithm of shell radius (in pc) for Group I shells (top panel) and for Group II shells (bottom panel). Filled circles mark shells that lie beyond 1.5 degrees in projection from the center of the SMC. Open symbols mark shells closer than 50 arcmin from the center of the SMC (in projection).

A first examination of these figures would imply that there is a lack of large shells (of either Group), with $\log r_s \geq 2.2$ pc, in the inner regions of the SMC (open symbols). However, after correcting for the different area fractions of the galaxy for the inner and outer regions, we find *no* statistically significant tendency of these larger shells to be located at larger galactocentric distances in the SMC.

An interesting feature of Figure 5 is that, in the inner

regions (open circles), there is a significant number of shells at intermediate radii, that show a large deviation towards higher expansion velocities, compared to the mean locus of the rest of the shells (i.e. above the line shown on the figure, to guide the eye). Quantitatively, the ratio of the number of group I inner shells (open circles) that lie above the marked line to the number of group I inner shells that lie below the line is 0.21 ± 0.05 , while the same ratio for the outer group I shells is significantly lower, at 0.06 ± 0.02 . For Group II shells, the picture is the same, but the number statistics are much poorer (the first ratio is 1 ± 0.08 and the second one 0.07 ± 0.05).

In the framework of the central source scenario, this surplus of faster expanding inner shells can be interpreted as a difference in the age distribution of shells, with the inner shells having a significant younger component, which would be expected since the inner parts of the SMC generally host younger populations (Maragoudaki et al. 2001). This option can only be considered for Group I shells. Viewed in a different way, the observed difference may indicate that for the same expansion velocity, shells in the inner regions tend to be smaller than the outlying ones, which could in principle result from the difference in the ambient density in the inner and outer regions (Tenorio-Tagle & Bodenheimer 1988), being higher in the former case. The fact that both Group I and Group II shells show very similar behavior (although the number statistics are very poor for Group II shells) in this respect, may indicate that the ambient density rather than age is the decisive factor, as it would seem meaningless to consider the ages of the central sources, if the central source scenario is not a valid option, at least for the Group II shells.

3.4 Search for evidence for cloud-disk collisions

As mentioned in the Introduction, some shell-like structures can result from the interaction of a high velocity cloud with the gaseous disk. Simulations show (Tenorio-Tagle et al. 1986; Rand & Stone 1996) that important morphological differences should be expected, between shells caused by stellar winds/SN explosions and cloud-disk collisions. While stellar wind/SN explosions shells evolve isotropically, shells caused by cloud-disk collisions grow preferentially in the direction of impact. Also, in the case of cloud-disk collisions, there is an absence of gas along the path of the cloud. In the case of M101 (van der Hulst & Sancisi 1988) some evidence exists for the high velocity debris gas from an ancient interaction

with a high velocity cloud. Therefore, it is relevant to investigate the morphological properties of Group II shells. However, close inspection of the data cubes for all 59 Group II shells did not reveal any HI features that might indicate past interaction with a high velocity cloud.

3.5 High Luminosity Shells

Group I and Group II shells have similar luminosities, lying within the range $\log L_s/n_0 \simeq -1.5$ to 5.8 (solar units) for Group I and between -1.4 and 5.1 for Group II shells. One might expect to find more high luminosity shells associated with OB associations (i.e. of Group I). However, that is not the case. The proportion of Group II high luminosity shells (with $\log L_s/n_0 \geq 3.5$) is the same (i.e. $\simeq 12\%$) as the proportion of Group I high luminosity shells.

We investigate here the spatial distribution of the most luminous shells, i.e. of those with $\log L_s/n_0 \geq 3.5$, of either Group. For Group I, these shells are evenly distributed in the main body of the SMC, but avoiding entirely the Wing region. The very luminous Group II shells are numbers 17, 21, 29, 36, 58, 59, 493 (shown as open squares on Figure 1). The first five of them are located close to each other in a region of the order of 1 degree in (projected) diameter in the North-Western (NW) outer regions of the SMC, where as was discussed in paragraph 3.1 there is also a large concentration of empty shells of all luminosities. This remarkable spatial coincidence may provide an important clue regarding the possible origin of these shells. From the remaining two shells, no. 493 is located in the NE outer regions, while no. 59 is one of the most remote South-Eastern shells.

The five high luminosity NW Group II shells appear to be, spatially and in radial velocity, associated with a chimney-like feature, located at the NW side. This feature has been described in Stanimirovic et al. (1999) as consisting of several aligned shells and filamentary structures. Interestingly, the ‘chimney’ starts its propagation in the direction almost perpendicular to the major kinematic axis of the SMC and turns to the North-East later on. It is ~ 550 pc wide. This reminds of Galactic chimneys, collimated HI structures thought to result from super-bubbles bursting out of the Galactic disk (Tomisaka & Ikeuchi 1987; Heiles et al. 1996). Even more interesting are several cometary-like clouds which appear to be associated with this NW feature in the position-velocity diagrams (as an example see Figure 6). The morphology of these clouds is similar to that of an atomic cloud associated with the W4 chimney (Taylor et al. 1999). This cloud, > 40 pc in size, was seen in ^{12}CO , 21cm line and continuum emission by Heyer et al. (1996), and is thought to be a result of photo-dissociation of molecular material by strong stellar winds from the stellar cluster that created the W4 chimney. The clouds that we find to be associated with the chimney-like feature in the SMC are larger, with a typical size of 150–300 pc.

To summarize, it is possible that the five very luminous NW Group II shells are associated with an ancient chimney in the SMC, and therefore they may be of different origin than other Group II shells. The question then rises, whether the rest of the Group II shells in the same NW region could also be associated with the same chimney.

Although this possible connection to an ancient chimney for several Group II shells seems to be an attractive

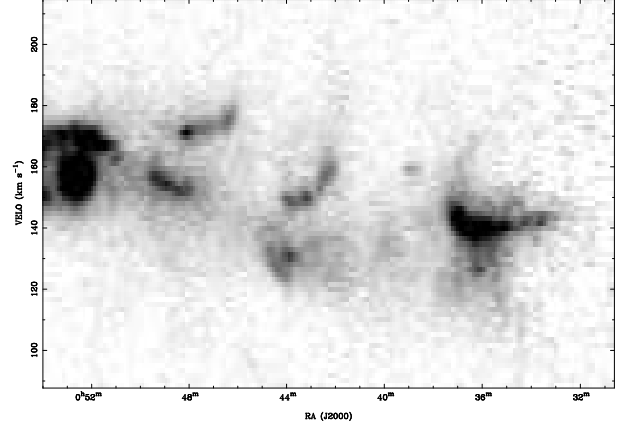


Figure 6. A position-velocity image of the SMC at Dec $-71^\circ 27' 11''$ (J2000), showing cometary clouds possibly associated with the chimney-like feature located around RA $00^h 40^m$.

alternative, it is by no means clear that it is a plausible explanation which can account for all of the shell properties. We note here that all of the 29 Group II shells that lie in this NW region are located right in the middle of the distribution of the rest of the shells of either group on the $\log v_s$ vs $\log r_s$ plane, actually following an even tighter relationship than the rest of Group II (or Group I) shells.

3.6 Summary of properties of Group I and Group II shells

(i) 12% of all expanding shells identified in the SMC, are of Group II, i.e. they do not appear to have an OB association or any other young stellar counterpart within their radius. Actually, many of them lie in regions where there are no young populations according to optical studies.

(ii) Group II shells lie preferentially in the outer regions. Part of this tendency may be caused by the fact that, in the inner regions, chance line-ups are more likely to mask the presence of an ‘empty’ shell.

(iii) Almost half of the Group II shells lie in the outer NW area of the SMC. There are indications that some of them could be connected to an old HI ‘chimney’ structure.

(iv) There is no convincing evidence that Group I and Group II shells differ morphologically in any systematic and significant way.

(v) Shell radius and expansion velocity differential distribution functions can be described by very similar power law fits, with $\alpha_{r_s} \simeq \alpha_{v_s}$. There are no significant differences between the values derived for the two different shell-groups, at least for the adopted lower limits of r_s and v_s used for the fits.

(vi) The distribution of both groups of shells on the $\log v_s$ vs $\log r_s$ plane is similar, with $v_s \propto r_s^{0.68 \pm 0.03}$ for Group I and $v_s \propto r_s^{0.87 \pm 0.08}$ for Group II shells.

4 THEORETICAL IMPLICATIONS

4.1 Standard model for evolution of shells

As mentioned briefly in the Introduction, the standard model for the evolution of giant shells (Weaver et al. 1977; McCray & Kafatos 1987) assumes that shell expansion is powered by stellar winds and, especially, by SNe from the parent OB association. It is also assumed that the input mechanical luminosity (L_s), dominated by SNe, remains constant with time. One way to compare properties of shells predicted by the standard model with observations is by deriving the differential shell-size or expansion velocity distribution functions and comparing them with the functions inferred from observations.

There are two main ingredients when trying to predict distribution functions $N(r_s)$ and $N(v_s)$: the spectrum of the input mechanical luminosity function (MLF), which is often considered either as a constant value or a power-law function ($\Phi(L_s) \propto L_s^{-\beta_{\text{ob}}}$), and the nature of shell creation, which could be either continuous (the case when shells are generated continuously at a constant rate), or a single burst (the case when all shells were created in an instantaneous burst). The slope β_{ob} of the MLF is related to the slope a of the HII luminosity function (HII LF), by $\beta_{\text{ob}} \leq a$. Hence, as a can be obtained from observations, it usually serves as an upper limit of β_{ob} . However, empirical measurements imply that one can easily assume $\beta_{\text{ob}} \simeq a$ in most cases (Oey & Clarke 1997). For the various combinations of the MLF function and the type of shell creation, one can derive the shell-size and expansion velocity distribution functions and compare them against observations (Fig.3, Table 3). In addition, the tight correlation between r_s and v_s (Section 3.3) prompted us to investigate the mean expansion velocity of an ensemble of shells, being at different stages of their evolution, \bar{v} as a function of shell size. We define \bar{v} as:

$$\bar{v}(r_0) = \frac{\sum_{r=r_0} v_i}{N(r_0)}. \quad (1)$$

Oey & Clarke (1997) derived $N(r_s)$ for three different cases within the standard adiabatic model. They considered growing shells, as well as stalled shells. The major result of their work was that $N(r_s) \propto r_s^{1-2\beta}$ is a robust description of the shell size distribution function for both continuous and instantaneous shell formation, for shells smaller than $\simeq 1300pc$. These shells are dominated by stalled shells. Shells larger than $\simeq 1300pc$, which are mainly growing shells, obey $N(r_s) \propto r_s^{4-5\beta}$. Oey & Clarke (1997) compared their predictions with observational data, particularly focusing on the SMC shell population (based on Staveley-Smith et al. 1997) as this was the most reliable and complete shell catalogue at the time. They found excellent agreement with the shell size distribution predicted by the theory, for the case of continuous formation and a power-law luminosity spectrum. In this scenario the shell size distribution was however dominated by stalled shells, while the shell catalogue they used (that of Staveley-Smith et al. 1997) only included growing shells: The latter authors did not catalogue stalled shells, but noted that there may be ~ 50 such shells in the SMC, only 10% of the total. Actually, *all shells* from the HI catalogue discussed in Section 2.1 have well defined expansion velocities. In addition, their dynamical ages are remarkably similar. Although mechanisms like shell re-acceleration may occur and result

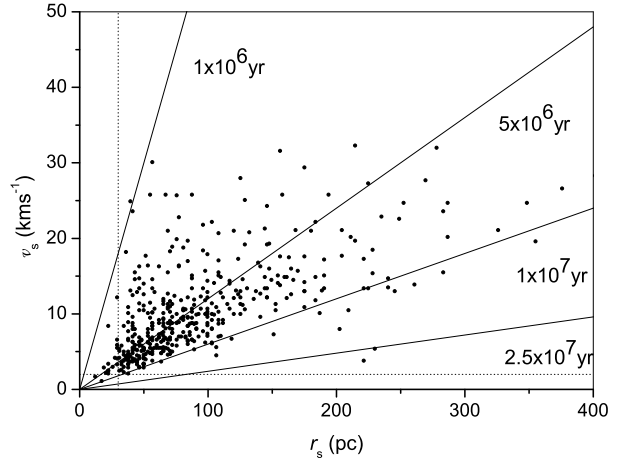


Figure 7. Expansion velocity versus shell radius diagram for HI shells that are found to have OB associations within their radius. The solid lines represent dynamical ages of 1, 5, 10 and 25 Myr. The horizontal and vertical dotted lines mark the resolution limits of the survey.

in shell ages being underestimated, it is hard to imagine that this (and/or other) process will work in accord on all shells to make the remarkably tight dynamical age distribution. It is possible that this points to a coherent burst of star formation that happened in the SMC. For these reasons, we repeat here calculations by Oey & Clarke (1997) but we only consider growing shells based on observational constraints. In addition, we derive the expansion velocity distribution and the mean expansion velocity for an ensemble of shells, which were not derived by Oey & Clarke.

4.1.1 Analytic expressions and comparison with observations

We start with equations for the growth of shells in a uniform ISM with a constant ambient density during the energy-conservation phase: $r_s \propto L_s^\gamma t^\alpha$ and $v_s \propto L_s^\gamma t^{\alpha-1}$ (MacLow & McCray 1988), where $\gamma = 1/5$ and $\alpha = 3/5$. Similarly to Oey & Clarke (1997) but considering *only* growing shells we derive $N(r_s)$, as well as $N(v_s)$ and $\bar{v}_s(r_s)$, in three different cases within the standard adiabatic model. In all three cases power-law behavior for all three functions can be expected.

(i) **Continuous creation, single luminosity.** Assuming that shells are continuously created, then:

$$\frac{dN}{dt} = \text{const.} = \psi. \quad (2)$$

If the input mechanical luminosity is the same for all shells, then:

$$\Phi(L_s) = \text{const.} = L. \quad (3)$$

As

$$N(r_s)dr_s = N(t)dt = \psi dt, \quad (4)$$

then substituting dr_s/dt we get:

$$N(r_s) \propto r_s^{1/\alpha-1}. \quad (5)$$

In a similar manner, starting with:

$$N(v_s)dv_s = N(t)dt = \psi dt, \quad (6)$$

and substituting $dv_s/dt \propto t^{\alpha-2}$, we derive:

$$N(v_s) \propto v_s^{-1+1/(\alpha-1)}. \quad (7)$$

Now,

$$\bar{v}(r_0) = \frac{\sum_{r=r_0} v_i}{N(r_0)} = \frac{r_0^{1/\alpha-1} N(r_0)}{N(r_0)}, \quad (8)$$

resulting in

$$\bar{v}_s \propto r_s^{1-1/\alpha}. \quad (9)$$

Substitution of the values for γ and α , results in:

$$N(r_s) \propto r_s^{2/3}, \quad (10)$$

$$N(v_s) \propto v_s^{-7/2}, \quad (11)$$

$$\bar{v}_s \propto r_s^{-2/3}. \quad (12)$$

(ii) **Single burst, luminosity spectrum.** If all shells were created at the same instant and the input mechanical luminosity has a power-law distribution then initial conditions are:

$$\Phi(L_s) \propto L_s^{-\beta_{\text{ob}}} r_s \propto L_s^\gamma t_0^\alpha \propto L_s^\gamma. \quad (13)$$

Starting with:

$$N(r_s)dr_s = N(L)dL = L_s^{-\beta_{\text{ob}}} dL. \quad (14)$$

Substituting $dr_s/dL \propto L_s^{-1}$, we derive:

$$N(r_s) \propto r_s^{(1-\beta_{\text{ob}})/\gamma-1}. \quad (15)$$

Similarly, $v_s \propto L_s^\gamma$, resulting in:

$$N(v_s) \propto v_s^{(1-\beta_{\text{ob}})/\gamma-1}. \quad (16)$$

Now,

$$\bar{v}(r_0) = \frac{\sum_{r=r_0} v_i}{N(r_0)} = \frac{v_0 N(r_0)}{N(r_0)} \propto r_0, \quad (17)$$

resulting in

$$\bar{v}_s \propto r_s. \quad (18)$$

Substituting values for γ and α , we get to:

$$N(r_s) \propto r_s^{4-5\beta_{\text{ob}}}, \quad (19)$$

$$N(v_s) \propto v_s^{4-5\beta_{\text{ob}}}, \quad (20)$$

$$\bar{v}_s \propto r_s. \quad (21)$$

Expectedly, eq.19 is in agreement with the result of Oey and Clarke (1997), for shells dominated by growing shells (shells larger than 1300pc, according to their analysis).

(iii) **Continuous creation, luminosity spectrum.** The last case considers continuous shell creation together with the power-law distribution with initial conditions given by:

$$\Phi(L_s) \propto L_s^{-\beta_{\text{ob}}} \frac{dN}{dt} = \text{const.} = \psi. \quad (22)$$

At one particular time, $t = t_0$:

$$N(r_s)\partial r_s = N(L)\partial L. \quad (23)$$

Substituting $L \propto r_s^{1/\gamma}/t_0^{\alpha/\gamma}$ we get to:

$$N(r_s) \propto r_s^{\frac{1-\gamma-\beta}{\gamma}} t_0^{\frac{\alpha(\beta-1)}{\gamma}}. \quad (24)$$

Now, total number of shells can be expressed with:

$$N(r_s) = \int_0^{t=t_{\text{max}}} r_s^{\frac{1-\gamma-\beta}{\gamma}} t^{\frac{\alpha(\beta-1)}{\gamma}} dt, \text{ or} \quad (25)$$

$$N(r_s) = r_s^{\frac{1-\gamma-\beta}{\gamma}} t_{\text{max}}^{\frac{\alpha(\beta-1)}{\gamma}+1}. \quad (26)$$

Shells expand in the ISM until they reach $v_s = v_{\text{ISM}}$, and at that stage $t_{\text{max}} = r_s/v_{\text{ISM}}$. Substituting this into the equation (25), we arrive at:

$$N(r_s) \propto r_s^{\frac{(1-\beta)(1-\alpha)}{\gamma}}. \quad (27)$$

And following the same reasoning we derive:

$$N(v_s) \propto v_s^{\frac{1}{\alpha-1}-1} \quad (28)$$

$$\bar{v}_s \propto r_s^{\frac{\alpha-1}{\alpha}}. \quad (29)$$

This corresponds to:

$$N(r_s) \propto r_s^{2(1-\beta_{\text{ob}})} \quad (30)$$

$$N(v_s) \propto v_s^{-7/2}, \text{ and} \quad (31)$$

$$\bar{v}_s(r_s) \propto r_s^{-2/3}. \quad (32)$$

We now compare these predictions with the functions inferred from observations (Section 3.3). Obviously, this comparison should be carried out for Group I shells that do appear to have young populations in them. However, the conclusions do not alter if all shells are considered, as Group II shells have very similar properties. According to the results described in Section 3, for all shells, $\bar{v}_s(r_s) \propto r_s^{0.71 \pm 0.03}$. This result rules out cases (i) and (iii) above. Also, the slopes for $N(r_s)$ and $N(v_s)$ were found to be very similar (cf Table 3), which, again is only satisfied by case (ii), indicating that at least the majority of the observed shells were created more or less in a single burst. This is also depicted on Figure 7, where we have overlaid on the v_s vs r_s data plane, lines of equal expansion age. It is obvious that most of the shells have dynamical ages close to 5 Myr (see also Paper I).

Since for case (ii), $\alpha_{r_s} = \alpha_{v_s}$, we can now use the observed mean slope $\alpha = (\alpha_{r_s} + \alpha_{v_s})/2 = -2.19 \pm 0.23$, to estimate the slope β_{ob} of the mechanical luminosity function for the SMC: $4 - 5\beta_{\text{ob}} = -2.19 \pm 0.23$, therefore, $\beta_{\text{ob}} = 1.24 \pm 0.05$. The slope of the HII LF estimated from observations is $a_{\text{obs}} = 2 \pm 0.5$ (Kennicutt, Edgar & Hodge 1989). Therefore, the condition $\beta_{\text{ob}} \leq a$ mentioned in Section 4.1 is satisfied.

To conclude, we have found that the shell radius and expansion velocity distributions of the SMC shells and supershells are consistent with the shells having been formed in a single burst and with an input mechanical luminosity spectrum $L_s^{-\beta_{\text{ob}}}$, with $\beta_{\text{ob}} = 1.24 \pm 0.05$, which is of the order of but smaller than the slope of the HII luminosity function, as it would be expected. Only growing shells were considered.

The same conclusions would be reached, if the distributions of Group II shells were considered instead of Group I. Actually, for Group II shells, $\bar{v}_s(r_s) \propto r_s^{0.87 \pm 0.08}$, with an exponent even closer to the case (ii) prediction, than Group I shells (which have a slope of 0.68 ± 0.03). This fact

is very difficult to understand within the framework of the standard model. One would have to assume that Group II shells are actually older (hence no young stars can be seen anymore within their radius), but they have somehow been re-accelerated. However, one would have to invoke a re-acceleration mechanism that would apply to all Group II shells in the same way and at the same time, to account for the tightness of the \bar{v}_s vs r_s relation and its similarity to the Group I relation.

4.2 Can Group II shells be GRB remnants ?

We investigate here the possibility that Group II (empty) shells are old remnants of GRBs. As mentioned in Section 1, recent studies suggest that the GRBs could leave shell-like remnants in the ISM (Efremov et al. 1998; Loeb & Perna 1998; Perna, Raymond & Loeb 2000). As it is not expected that the GRB remnants would be associated with young stellar objects this could be one possible explanation for Group II shells. In turn, finding GRB remnants is very important as it would help to constrain types of environments where GRBs occur and hence the GRB formation mechanisms.

The underlying source, connected to a GRB event, that produces the initial explosion, releasing a large amount of kinetic energy into the surrounding medium, is still unknown. The most common theory is based on the collapse of a single super-massive star (Paczynski 1998), so called ‘collapsar’ scenario. An alternative scenario involves a coalescence of two compact objects, either two neutron stars in a binary system or a neutron star and a black hole (Eichler et al. 1989). As massive stars have short lives it is expected that their remnants should be found in dense environments. On the other hand, merging neutron stars are old objects and their remnants are expected in intermediate to low-density environments (Perna, Raymond & Loeb 2000). It is believed that most of the GRBs are beamed. The most recent results by Bloom, Frail, & Kulkarni (2003) suggest an extremely narrow range for the typical amount of energy that GRBs deposit in the ISM: $8 \times 10^{50} - 5 \times 10^{51}$ ergs, after correction for the beaming effect.

GRB remnants display a characteristic double-shell morphology during the intermediate age of < 5 kyr (Ayal & Piran 2001) which distinguishes them from the OB shell remnants (resulting from stellar winds and multiple supernovae explosions). At later stages of their evolution GRB shells are very similar to typical OB shells. Perna, Raymond & Loeb (2000) suggested several spectral and/or abundance signatures for their identification. The only small difference between OB shells and GRB shells at the later stages of evolution is in the nature of their growth: while most of the growth of OB shells occurs due to the energy conservation resulting from a continuous fueling by supernovae bursts, being described by the Sedov-Taylor phase, GRB shells expand mostly as a result of momentum conservation, which is described as the snowplough phase. Hence, the expansion of GRB shells can be expressed in a similar way to the expansion of OB shells (discussed in Section 4.1).

Based on equations for the swept-up shell once it enters the snowplough phase given by Cioffi, McKee, & Bertschinger (1988), the growth of a GRB-created shell in an uniform ISM can be described by: $r_s \propto L_s^\gamma t^\alpha$ and $v \propto L_s^\gamma t^{\alpha-1}$, where $\gamma = 0.22$ and $\alpha = 0.30$. On the observed

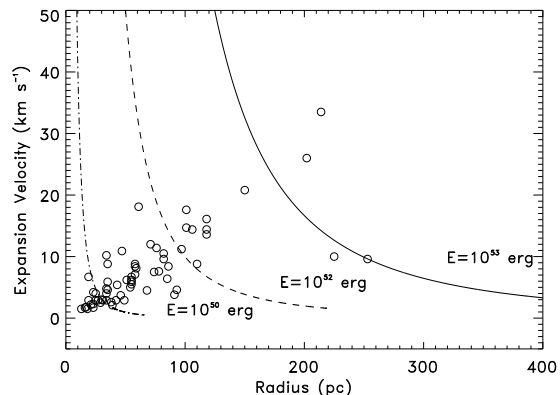


Figure 8. Comparison of observations of empty shells (open circles) with predictions of the GRB model for the expansion velocity versus shell radius relation.

r_s vs v_s relation for Group II shells, we overlaid three equal energy curves for GRB-created shells (Figure 8). Only shells with energies in the range of $8 \times 10^{50} - 5 \times 10^{51}$ ergs can be considered as candidates for GRB-created shells, as mentioned earlier. The diagram in Fig. 8 shows that there are about 15–20 such shells. Their mean age is (5 ± 2) Myr. The rest of the Group II shells have sizes and expansion velocities too small or too large to be explained by GRB explosions. Now, if all of the 15–20 shells were caused by GRBs, one would infer a GRB rate of $3\text{--}4 \text{ Myr}^{-1}$, which is consistent with the predicted frequency of GRBs in any galaxy by Schmidt (1999), for a beaming factor of ~ 0.03 . Of course the value inferred here should be treated as a lower limit, because the sample of empty shells suffers from severe incompleteness, as such shells cannot be identified in dense regions due to chance line-ups. Note also the inhomogeneity in the spatial distribution of Group II shells in the SMC (Fig. 1).

We compare now the estimated GRB rate in the SMC, from the potential GRB remnants, with the predictions based on the ‘collapsar’ scenario. The estimated rate of Type II supernovae in the SMC is (500 ± 300) per Myr (Crawford et al. 2000). MacFadyen & Woosley (1999) showed that collapsars are only a small fraction of all supernovae, approximately 1%. Hence, the collapsar rate in the SMC can be estimated as (5 ± 3) per Myr. This agrees well with the previously estimated (lower limit) GRB rate. However, being associated with deaths of the most massive stars, collapsars should be found in the regions with recent active star-formation, while the great majority of the ‘empty’ shells are found in low-density environments with no young populations. Therefore, although the statistics are encouraging, it is unlikely that the shells in question have their origin in collapsars.

Looking into the alternative ‘merger’ scenario, the coalescence rate of neutron stars in our Galaxy was estimated to be 17 per Myr (Phinney 1991). Scaling this number by the ratio of potentially observable pulsars in the Galaxy and in the SMC, which is equal to 0.03, gives an estimate of the coalescence rate of neutron stars in the SMC of approximately 1 per Myr. This is lower than the estimated rate, which is in any case a lower limit. However, because the empty shells

in question lie in an old stellar environment, it cannot be ruled out that at least some of them, about 5 in number if we adopt the neutron star coalescence rate given above, could be the result of a merger GRB.

In conclusion, the mechanical luminosities of about 15–20 Group II shells are consistent with the shells being GRB remnants, thus suggesting a GRB rate of ≥ 4 per Myr in the SMC, which is consistent with an estimate of the number of GRBs from the collapse of super-massive stars. However, the latter would require active recent star formation in the neighborhood of the shells, which is not the case. On the other hand, GRBs caused by neutron star coalescence occur in old stellar populations and could account for about 5 of the Group II shells.

4.3 Turbulence

As mentioned in Section 1, the non-linear evolution of a self-gravitating disk can also lead to formation of shells, that are not related to a central energy source (Wada & Norman 1999). As Elmegreen (1997) also suggested, HI ‘bubbles’ (or shells) could result naturally from the turbulent nature of the interstellar medium, i.e. it is possible that most of the structure of the ISM is the result of natural gaps and holes in the fractal gas distribution caused by turbulence. Even if turbulence alone cannot produce the required expansion velocities, it is possible that supernovae, stellar winds and ionizing radiation fill these gaps with ionized gas and provide additional internal pressure. There is no modelling to date of the relation between expansion velocity and size of shells formed by turbulence. But one might expect (Elmegreen 2000, private communication) that the expansion velocity would be approximately proportional to the square root of the shell radius ($v_s \propto r_s^{0.5}$), because that is about what is seen for turbulence in general, i.e., for the scaling of clouds and collections of clouds. Observationally we found that all shells observed follow the relation $v_s \propto r_s^{0.71 \pm 0.03}$, which is close to the previous qualitative statement. If most shells are indeed caused by turbulence, that would explain why there is a relatively weak correlation with OB associations and why the properties of “empty” and “non-empty” shells are not very different in most cases.

Recently, Dib & Burkert (2004) have investigated whether the observed shells in the ISM of Holmberg II could be produced by turbulence. Numerical simulations were performed for different types of turbulent driving while taking into account thermal and gravitational instabilities. It appears that turbulence driven on large scales, rather than supernova explosions, can reproduce observed shells and holes in Holmberg II located in regions without any detected stellar activity. Future progress, as well as detailed comparison with observations, in this direction is eagerly awaited.

4.4 The role of the environment

As was mentioned in the Introduction, regardless of the origin of a shell, its evolution can be also affected by external factors: radiation pressure from field stars (which is important for supergiant shells), the density of the ambient ISM and its inhomogeneities, interactions between shells, globular cluster passage, etc. It is not clear, however, how one

could quantitatively identify observational signatures of such processes, in order to proceed to a quantitative verification of their action and relative importance. We described in Section 3.2.1 the difference in the behavior of inner and outer shells (of either Group I or II) which could be accounted for by the difference in the ambient density. We also noted that there is an indication (Section 3.2) that larger shells follow a shallower linear correlation on the $\log v_s - \log r_s$ plane than smaller shells. This could be the effect of age (with larger shells being older), combined with environmental factors. This latter statement however, is purely conjectural at this stage and has to be further investigated in the future.

5 SUMMARY AND CONCLUSIONS

There are 509 HI shell structures in the SMC, all apparently very young, with dynamical ages of a few Myr. We have found that 59 of these shells are empty, in the sense that they have no young stellar objects associated with them. It is shown in Section 3 that on the whole properties of empty and non-empty shells are very similar. Besides several individual cases, there is nothing significantly different in shell properties -other than selection biases- that could point to a different origin for these two groups of shells. The reason could be a similar origin for all shells in the SMC and/or a great importance that environmental effects play in shaping shell characteristics especially at later stages of evolution.

The shell radius and expansion velocity distribution functions are consistent with the standard model, if all shells were created in a single burst and the input mechanical luminosity had a power-law distribution. This would indicate a burst of star formation at a particular epoch (about 5 Myr ago). This interpretation however cannot explain why the 59 shells with no young stellar counterparts show almost exactly the same behavior as shells with OB associations within their radius.

Sizes and expansion velocities for about 15–20 empty shells are consistent with the expected properties for GRB remnants. These shells suggest a GRB rate of >4 per Myr in the SMC, which is consistent with the predicted frequency of GRBs by Schmidt (1999) for a beaming factor of ~ 0.03 , as well as with an estimate of the number of GRBs from a collapse of super-massive stars. However, the latter would require active recent star formation in the neighborhood of the shells, which is not the case. The other possibility is merger GRBs which requires an old stellar environment. However, the predicted frequency of such events is too low to account for more than $\simeq 5$ of the 15–20 empty shells in question. The rest of the empty shells have sizes and expansion velocities too low or too high to be explained by GRB explosions. So, on the whole, only a small number of the empty shells may have been formed by GRBs.

We have also searched for morphological signatures that would indicate a possible collision with a high velocity cloud for “empty” shells. No significant features were found.

Most of the high luminosity empty shells appear to be associated with a chimney-like feature in the NW outer regions of the SMC.

A comparison of the properties of shells lying in the inner and outer regions of the SMC indicated that the density

of the environment within which a shell is expanding might be significantly affecting the evolution of a shell.

Therefore, none of the mechanisms described in the introduction and examined here, can fully account for the properties of all of the shells. Turbulence is a promising mechanism for the initiation of shells, but detailed comparison with the observations was not possible at this stage, due to lack of detailed models.

Acknowledgements S. Stanimirovic was partially supported by NSF grants AST-0097417 and AST-9981308, during this research. The authors would also like to thank B. Elmegreen, Ch. Goudis, V. Kalogera and R. Perna for useful discussions.

REFERENCES

- Ayal S., Piran T., 2001, ApJ, 555, 23
- Azzopardi M., Breysacher J., 1979, A&A, 75, 120
- Bica E.D., Schmitt H.R., 1995, A&AS, 101, 41
- Bloom J.S., Frail D.A., & Kulkarni S.R., 2003, ApJ, 594, 674
- Brinks E., Bajaja E., 1986, A&A, 169, 14
- Bureau M., Carignan C., 2002, AJ, 123, 1316
- Cioffi D.F., McKee C.F., Bertschinger E., 1988, ApJ, 334, 252
- Crawford F., Gaensler B.M., Kapsi V.M., Manchester R.N., Camilo F., Lyne A.G., Pivovarov M.J., 2001, ApJ, 554, 152
- Dib S., Burkert A., 2004, ApJ, submitted (astro-ph/0402593)
- Eichler D., Livio M., Piran T., Schramm D.N., 1989, Nature, 340, 126
- Efremov, Y. N., Ehlerova S., Palous J., 1999, ApJ, 350, 457
- Efremov Y. N., Elmegreen B. G., Hodge P. W., 1998, ApJ, 501, 163L
- Elmegreen B.G., Chiang W.-H., 1982, ApJ, 253, 666
- Elmegreen B.G., 1997, ApJ, 477, 196
- Elmegreen B.G., Hunter, D., 2000, ApJ, 540, 814
- Filipovic M.D., Haynes R.F., White G.L., Jones P.A., 1998, A&AS, 130, 421
- Gardiner L.T., Hatzidimitriou D., 1992, MNRAS, 257, 195
- Harris J. & Zaritsky D., 2004, AJ, 127, 1531
- Heiles C., Reach W. T., Koo B.-C., 1996, ApJ, 466, 191
- Heiles, C. 1984, ApJSuppl, 55, 585
- Heyer M. H., Brunt C., Snell R. L., Howh J., Schloerb F. P., Carpenter J. M., Normandeau M., Taylor A. R., Dewdney P. E., Cao Y., Terebey S., Beichman C. A., 1996, ApJ, 464, L175
- Kennicutt R.C., Edgar B.K., Hodge P.W., 1989, ApJ, 337, 761
- Kim S., Dopita M.A., Staveley-Smith L., & Bessell M.S., 1999, AJ, 118, 2797
- Kontizas E., Morgan D.H., Kontizas M., Dapergolas A., 1988, A&A, 201, 208
- Loeb A., Perna R. 1998, ApJ, 503, 35L
- MacFadyen A.I., Woosley S.E., 1999, ApJ, 524, 262
- MacLow M., McCray R., 1988, ApJ, 324, 776
- Maragoudaki F., Kontizas M., Morgan D.H., Kontizas E., Dapergolas A., Livanou E., 2001, A&A, 379, 864
- Mathewson D.S., Ford V.L., Visvanathan N., 1987, ApJ, 333, 617
- Maurice E., Bouchet P., Martin N., 1989, A&AS, 78, 445
- McClure-Griffiths N.M., Dickey J.M., Gaensler B.M., Green A.J., Haynes R.F., Wieringa M.H., 2000, AJ, 119, 2828
- McCray R., Kafatos M., 1987, ApJ, 317, 190
- Morgan D.H., Vassiliadis E., Dopita M.A., 1991, MNRAS, 251, 51
- Muller E., Staveley-Smith L., Zealey W., Stanimirovic S., MNRAS, 339, 105
- Oey M. S., Clarke, C. J., 1997, MNRAS, 289, 570
- Oey M. S., Clarke, C. J., 1999, In Proceedings of the 2nd Guillermo Haro Conference “Interstellar Turbulence”, eds. J. Franco and A. Carraminana, Cambridge U. Press, p. 112
- Paczynski B., 1998, ApJ, 494, 45L
- Perna R., Raymond J., 2000, ApJ, 539, 706
- Perna R., Raymond J., Loeb A., 2000, ApJ, 533, 658
- Phinney E.S., 1991, ApJ, 380, L17
- Puche D., Westpfahl D., Brinks E., Roy J.R., 1992, AJ, 103, 1841
- Rand R. J., Stone J. M., 1996, AJ, 111, 190
- Rhode K.L., Salzer J.J., Westpfahl D.J., Radice L.A., 1999, AJ, 118, 323
- Savage A., Waldron I.D., Morgan D.H., Tritton S.B., Cannon R.D., Dawe J.A., Bruck M.T., Beard S.M., Palmer J.B., 1985a, The UK Schmidt Telescope Objective Prisms: II. Illustrations of objective Prism Spectra, Royal Observatory, Edinburgh
- Savage A., Waldron I.D., Fretwell M., Morgan D.H., Tritton S.B., Cannon R.D., Bruck M.T., Beard S.M., Palmer J.B., 1985b, The UK Schmidt Telescope Objective Prisms: III. Illustrations of objective Prism Spectra, Royal Observatory, Edinburgh
- Schmidt M., 1999, ApJ, 523L, 117
- Shostak G.S. & Skillman E.D., 1989, A&A, 214, 33
- Stanimirovic S., 1999, PhD Thesis, University of Western Sydney Nepean
- Stanimirovic S., Staveley-Smith L., Dickey J.M., Sault R.J., Snowden S.L., 1999, MNRAS, 302, 417
- Staveley-Smith L., Sault R.J., Hatzidimitriou D., Kesteven M.J., McConnell D., 1997, MNRAS, 289, 225
- Stewart S.G., Walter F., 2000, AJ, 120, 1794
- Taylor A. R., Irwin J. A., Matthews H. E., Heyer M. H., 1999, ApJ, 513, 339
- Tenorio-Tagle G., 1981, A&A, 94, 338
- Tenorio-Tagle G., Bodenheimer P., Rozyczka M., Franco J., 1986, A&A, 170, 107
- Tenorio-Tagle G., Bodenheimer P., 1988, ARAA, 26, 145
- Tomisaka K., Ikeuchi S., 1987, PASJ, 38, 697
- van der Hulst T., 1996, in The Minnesota Lectures on Extragalactic Neutral Hydrogen ASP Conference Series, E.D. Skillman, ed., 106, 47
- van der Hulst T., Sancisi R., 1988, AJ, 95, 1354
- Wada K., Norman C.A., 1999, ApJ, 516L, 13
- Wada K., Spaans M., Kim S., 2000, ApJ, 540, 797
- Wallin J.F., Higdon J.L., Staveley-Smith L., 1996, ApJ, 459, 555
- Walter F. & Brinks E., 1999, AJ, 118, 273
- Wang Q., Wu X., 1992, ApJSuppl, 78, 391
- Weaver R., McCray R., Castor J., Shapiro P., Moore R., 1977, ApJ, 218, 377
- Wilcots E.M. & Miller B.W., 1998, AJ, 116, 2363
- Zaritsky D., Thompson, I.B., Grebel E.K., Massey P., 2002, AJ, 123, 855